Journal Pre-proofs

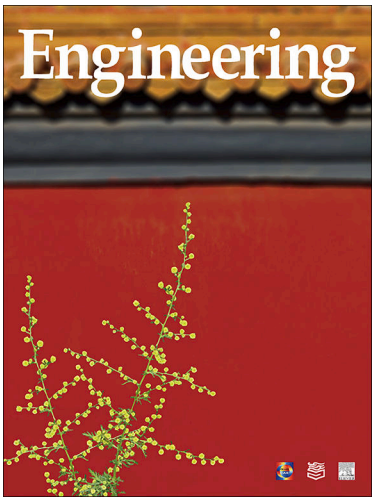

Article

Big Geodata Reveals Spatial Patterns of Built Environment Stocks Across and Within Cities in China

Zhou Huang, Yi Bao, Ruichang Mao, Han Wang, Ganmin Yin, Lin Wan, Houji Qi, Qiaoxuan Li, Hongzhao Tang, Qiance Liu, Linna Li, Bailang Yu, Qinghua Guo, Yu Liu, Huadong Guo, Gang Liu

PII: S2095-8099(23)00271-0
DOI: https://doi.org/10.1016/j.eng.2023.05.015
Reference: ENG 1303

To appear in: *Engineering*

Received Date: 16 October 2022
Revised Date: 15 May 2023
Accepted Date: 16 May 2023

Please cite this article as: Z. Huang, Y. Bao, R. Mao, H. Wang, G. Yin, L. Wan, H. Qi, Q. Li, H. Tang, Q. Liu, L. Li, B. Yu, Q. Guo, Y. Liu, H. Guo, G. Liu, Big Geodata Reveals Spatial Patterns of Built Environment Stocks Across and Within Cities in China, *Engineering* (2023), doi: https://doi.org/10.1016/j.eng.2023.05.015

Civil Engineering—Article

Big Geodata Reveals Spatial Patterns of Built Environment Stocks Across and Within Cities in China

Zhou Huang [a,b,*,#], Yi Bao [a,b,#], Ruichang Mao [c,d,#], Han Wang [a], Ganmin Yin [a], Lin Wan [e], Houji Qi [a], Qiaoxuan Li [f], Hongzhao Tang [g], Qiance Liu [c,h], Linna Li [i], Bailang Yu [f], Qinghua Guo [a], Yu Liu [a], Huadong Guo [b,j,*], Gang Liu [k,*]

[a] *Institute of Remote Sensing and Geographical Information Systems, School of Earth and Space Sciences, Peking University, Beijing 100871, China*

[b] *International Research Center of Big Data for Sustainable Development Goals, Beijing 100094, China*

[c] *SDU Life Cycle Engineering, Department of Green Technology, University of Southern Denmark, Odense 5230, Denmark*

[d] *Department of Construction Management, School of Civil Engineering, Tsinghua University, Beijing 100084, China*

[e] *School of Computer Science, China University of Geosciences, Wuhan 430074, China*

[f] *School of Geographical Sciences, East China Normal University, Shanghai 200062, China*

[g] *Land Satellite Remote Sensing Application Center, Ministry of Natural Resources, Beijing 100048, China*

[h] *Institute of Geographic Sciences and Natural Resources Research, Chinese Academy of Sciences, Beijing 100101, China*

[i] *Department of Geography, California State University, Long Beach, California 90840, USA*

[j] *Aerospace Information Research Institute, Chinese Academy of Sciences, Beijing 100094, China*

[k] *College of Urban and Environmental Sciences, Peking University, Beijing 100871, China*

[#] These authors contributed equally.
*Corresponding authors.
Email addresses: huangzhou@pku.edu.cn (Z. Huang); hdguo@radi.ac.cn (H. Guo); gangliu@pku.edu.cn (G. Liu).

Abstract

The patterns of material accumulation in buildings and infrastructure accompanied by rapid urbanization offer an important, yet hitherto largely missing stock perspective for facilitating urban system engineering and informing urban resources, waste, and climate strategies. However, our existing knowledge on the patterns of built environment stocks across and particularly within cities is limited, largely owing to the lack of sufficient high spatial resolution data. This study leveraged multi-source big geodata, machine learning, and bottom-up stock accounting to characterize the built environment stocks of 50 cities in China at 500 m fine-grained levels. The per capita built environment stock of many cities (240 tonnes per capita on average) is close to that in western cities, despite considerable disparities across cities owing to their varying socioeconomic, geomorphology, and urban form characteristics. This is mainly owing to the construction boom and the building and infrastructure-driven economy of China in the past decades. China's urban expansion tends to be more "vertical" (with high-rise buildings) than "horizontal" (with expanded road networks). It trades skylines for space, and reflects a concentration–dispersion–concentration pathway for spatialized built environment stocks development within cities in China. These results shed light on future urbanization in developing cities, inform spatial planning, and support circular and low-carbon transitions in cities.

Keywords: urban system engineering, built environment stock, spatial pattern, urban sustainability, big geodata

1. Introduction

Urbanization is one of the most important global megatrends of the past century [1,2]. The next three decades will see another 2.5 billion rural residents moving into urban areas—90% of them being from Asia and Africa—and approximately 68% of the global population will live in cities by 2050 [3]. Urbanization represents a process of population concentration [4], expansion of construction land [5], together with the accumulation of materials in buildings [6] and infrastructure [7] (built environment) that defines the physical space of urban activities and provides key services such as shelter and mobility [8]. The construction, maintenance, and demolition of urban built environment stocks result in major sustainability challenges for cities [9–11], such as resource demand [12], energy use [13], greenhouse gas (GHG) emissions [14,15], and construction and demolition waste generation [16]. Therefore, understanding the patterns of urban built environment stock development is important to facilitate urban system engineering, inform the circular and low-carbon transition of existing cities, and shed

light on future urbanization in the Global South [17].

Pr ales, particularly for the temporal dynamics of key construction materials, such as steel [18,19] and cement [20], and sectors, including buildings [21] and subways [22]. A handful of efforts were made at the urban scale [23–25]; however, our existing knowledge of the spatial patterns of built environment stocks across and particularly within cities is limited, largely owing to the lack of high spatial resolution data—which is highly data- and labor-intensive [26]. Emerging new types of urban big data, such as point-of-interest data [27], and technologies, such as remote sensing and deep learning [28], offer an opportunity to address such gaps. However, this is not fully captured in the literature.

China is a living laboratory for global urbanization over the past four decades [29]. It has experienced a boom in the development of urban built environment stocks. This benefits economic growth and the well-being of urban residents in China. It also results in significant environmental challenges, including construction and demolition waste generation [16,30], and GHG emissions [31,32]. A thorough benchmarking and understanding of built environment stocks across and within cities at different levels of development is essential for China's endeavor to improve the quality of new urbanization, build zero-waste and eco-cities, and achieve its climate ambition of "peaking before 2030 and neutrality before 2060." However, existing characterization of built environment stocks for Chinese cities either focus on specific construction materials [24] or sectors [33–35] without spatial resolution, or are limited to a few cities, such as Beijing [36] and Shanghai [37], or urban areas, such as Tiexi District of Shenyang [38], that cannot support cross-city comparison.

Here, we aimed to address these knowledge gaps by leveraging various urban systems engineering methods involving big geodata, machine learning, and bottom-up stock accounting. We quantified the built environment stocks of 50 Chinese cities and explored their spatial patterns across and within them. Our findings help to inform waste management, urban mining, climate change mitigation, and spatial planning, and the circular and low-carbon transition of Chinese cities, shedding further light on the sustainable urban development of other cities worldwide.

2. Materials and methods

The overall workflow for characterizing the spatialized built environment stocks of the 50 cities in China is shown in Fig. 1. Briefly, multi-source geodata was initially collected and the material composition intensity (MCI) database was established, followed by leveraging bottom-up stock accounting and machine learning approaches to calculate gridded building and infrastructure material stocks of 50 Chinese cities on 500 m fine-grained levels. Finally, a spatial analysis was conducted to reveal the pathway for spatialized urban built environment stock development across and within cities in China.

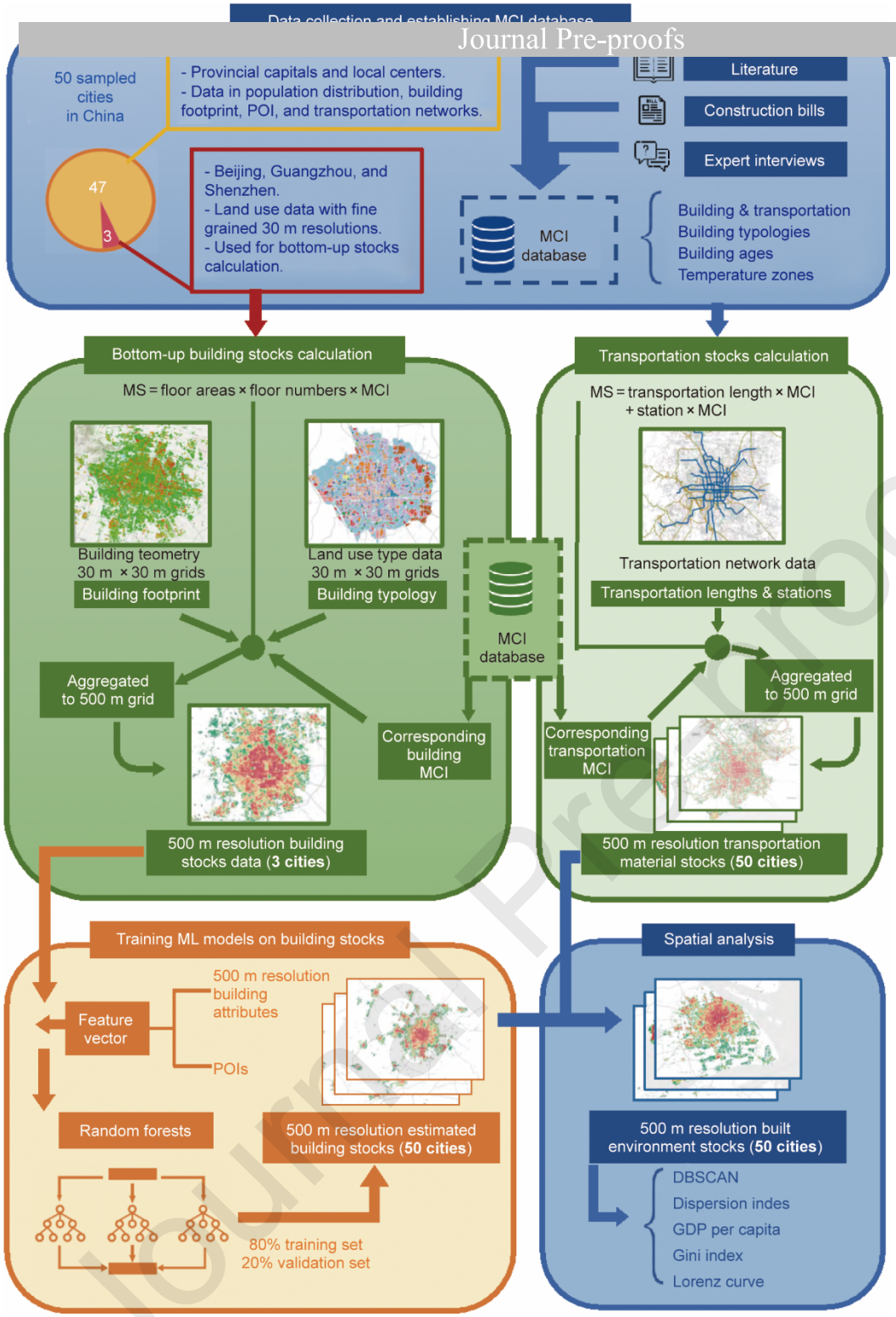

Fig. 1 Study design and workflow for characterizing the built environment stocks of 50 cities in China at 500 m fine-grained levels. MCI: material composition intensity; POI: points of interest; MS: material stock; GDP: gross domestic product; ML: machine learning; DBSCAN: density-based clustering algorithm

2.1 Scope and data sources

The built environment stocks considered in this analysis included different types of buildings, such as agricultural, commercial, educational, historical, industrial, mixed, municipal, parking, public, residential, sports, and storage, and transport infrastructure, including roads, railways, and subways. Other types of infrastructure including ports and pipelines contribute very little to the total urban built environment stock and are considered negligible. The year of reference for the calculation was 2018; it was largely based on the availability of multisource big geodata, and 50 Chinese cities were selected for analysis. They cover all provincial capitals and cities of economic, cultural, and location importance. Together, they account for 50% of the gross domestic product (GDP), 32% of the population, and 15% of the built-up land area of all cities in China, and are deemed representative and sufficient for our comparison.

The important datasets of these 50 selected cities include building footprints—from Baidu, the largest online map portal in

China, building age—mainly from real-estate company websites, land use—on a 500 m resolution for five land use categories from [redacted] hou, and Shanghai) that are based on a 30m fine-grained level for 12 land use categories, points of interest (POIs)—from Amap, the largest mobile online map platform in China, transport infrastructure—mainly from OpenStreetMap, gridded population—from WorldPop mainland China dataset [40], socioeconomic development—mainly from the municipal statistical yearbook, and MCI data collected from various sources (Supplementary Material Sections S1.1–1.6).

In particular, a China-specific building MCI database was compiled from various sources, including the bills of quantities, expert interviews, and literature, covering over 2000 sample buildings constructed between 1963 and 2017. They were classified into 12 building typologies (agricultural, commercial, educational, historical, industrial, mixed, municipal, parking, public, residential, sport, and storage). The road and subway MCIs were collected from construction bills provided by several construction companies in China (Supplementary Material Section S1.7).

2.2 Bottom-up and spatially refined building stocks of three sample cities

Three cities, Beijing, Guangzhou, and Shanghai, were selected as the training samples based on data availability. In particular, the 12 building types from 30 m fine-grained land use data were collected the three cities from the corresponding municipal planning administrations (Supplementary Fig. S2). A bottom-up and spatially refined building stock accounting method was used for these three cities, based on our previous study [36] and shown in Eq. (1). Ten types of construction material were considered: cement, steel, timber, brick, gravel, sand, asphalt, lime, glass, and ceramic.

$$MS_{m,i} = \sum_{m,i}(BF_i \times NF \times MCI_{m,i}) \#(1)$$

$MS_{m,i}$ represents the building stock of material m present in building type i, BF_i (measured in m^2) is the area of the one-floor building footprint, NF represents the number of building floors, and $MCI_{m,i}$ ($kg \cdot m^{-2}$) is the composition intensity of material m of type i.

2.3 Machine learning for estimating building stocks for the other 47 cities

Accurate building data with attributes of function, year of construction, and 30 m fine-grained land use data were unavailable for the other 47 cities. Therefore, we leveraged machine learning models to estimate building stocks using the gridded stock values of the three training sample cities aggregated at a 500 m resolution. We combined building attributes and POI attributes to encode each grid with a vector and utilized the random forest model to build the mapping from the grid vector to its material stocks. The model was trained using 80% of the data from Beijing, Guangzhou, and Shenzhen, validated using the remaining 20%, and eventually applied to estimate the building material stock values for each grid of the other 47 cities.

2.4 Transportation material stock calculation

The material stock value was computed for the urban transportation systems in all 50 cities based on the lengths and MCIs of railways, subways, and roads, as shown in Eq. (2). Road MCIs cover five levels: expressways, first-, second-, third-, and fourth-class roads. Railway lines, subway lines, and subway stations were considered for the railway and subway stock estimation.

$$MS_{m,j} = \sum_{m,i}(TL_j \times MCI_{m,j}) + (S \times MCI_{m,s}) \#(2)$$

$MS_{m,j}$ is the transportation stock of material m in the transportation construction sector j (road, railway, and subway), TL_j is the length of transportation (measured in m) in sector j and $MCI_{m,j}$ is the composition intensity of material m in sector j (measured in $kg \cdot m^{-1}$). S is the subway station, and $MCI_{m,s}$ is the composition intensity of material m in subway station s.

2.5 Spatial statistics for pattern identification

Material stock and population values were used from 500 m × 500 m grids for pattern identification in spatial statistics (Supplementary Material Section S3). The grids with the top 1% stock values are regarded as building stock centers. A density-based clustering algorithm (DBSCAN) [41] was used to aggregate the high-stock grids together (Section S3.1). The dispersion index was calculated for each DBSCAN cluster to quantify the spatial dispersion of grids (Section S3.2). The city-level building stock per capita was calculated to understand the role of economic development. The unevenness of the grid-level building stock was determined using the Gini coefficient and the Lorentz curve (Section S3.3). Fitting the grid stock distribution of all 50 cities showed that they conformed to a two-parameter exponential distribution regardless of size, location, and economic development levels (Section S3.4).

3. Results and discussion

3.1 Patterns of urban built environment stocks across cities

The urban built environment stocks of 50 Chinese cities increased to 110 Gt in 2018, which is larger than the total global reso erial stock, whereas other infrastructure only contributed a small share (2.3%). Nonmetallic minerals represented by gravel (51 Gt), cement (26 Gt), sand (17 Gt), and brick (12 Gt) were responsible for 96% of the total types of materials. Steel (1.9 Gt), timber (0.6 Gt), lime (0.5 Gt), and other materials (totaling 1.0 Gt) were used in relatively low quantities (Supplementary Figure Fig. S10).

The total urban built environment stock ranged from 350 Mt in Lhasa to 6786 Mt in Beijing when compared across cities. Stock quantities in 49 out of 50 Chinese cities (2202 Mt on average; except for Lhasa with 350 Mt) and stock densities (4.97 $t \cdot m^{-2}$ on average) in all 50 Chinese cities were substantially higher than in many western cities—for example, 67 Mt and 0.22 $t \cdot m^{-2}$ in Odense [12], and 380 Mt and 0.96 $t \cdot m^{-2}$ in Vienna [43], while per capita stocks (249 tonnes per capita ($t \cdot cap^{-1}$) in China) were at approximately the same level—329 $t \cdot cap^{-1}$ in Odense [12], 247 $t \cdot cap^{-1}$ in Wakayama [12], 210 $t \cdot cap^{-1}$ in Vienna [43], 209 $t \cdot cap^{-1}$ in Padua [44], and 272 $t \cdot cap^{-1}$ in the United Kingdom [45] (Supplementary Table S19). These differences could be explained by the large size and population, but limited built-up area in most Chinese cities [46], together with construction-driven urbanization and real estate-based economic development in the past decades [47].

The urban built environment stocks were unevenly distributed across Chinese cities with varying levels of socioeconomic development (Fig. 2 and Supplementary Figs. S11–14). Cities with large stocks were mostly distributed in the east (35.88%), north (18.58%), and southwest (11.66%), whereas relatively lower amounts were found in cities in the south (9.74%), northeast (9.56%), central (9.11%), and northwest (5.46%) (Supplementary Fig. S15). In particular, the top 10 cities with the largest stocks were all distributed in China's major urban agglomerations. This includes 3.3 Gt in Hangzhou and 6.8 Gt in Beijing, represented by 25.9 Gt in the Yangtze River Delta and 17.9 Gt in Jing–Jin–Ji Metropolitan Region, which account for 62% of the total. However, cities in the northeast (323 $t \cdot cap^{-1}$, 3.8 $kg \cdot CNY^{-1}$) and northwest (346 $t \cdot cap^{-1}$, 4.0 $kg \cdot CNY^{-1}$) show significantly higher values than other regions (Supplementary Fig. S16) on a per capita level and per GDP level. This was mainly related to the shrinking population in the northeast [48] and the low population density in the northwest [49], suggesting that material occupancy does not translate into economic growth in these areas [50]. A consideration of the built-up areas shows that cities in the north have the densest stocks (6.1 $t \cdot m^{-2}$), while the southwest and northwest have lower stock density (both approximately 4.0 $t \cdot m^{-2}$ on average, Fig. S16). This reflects the geomorphological and socioeconomic characteristics of western China, which has more abundant land and less dense populations than the east [51].

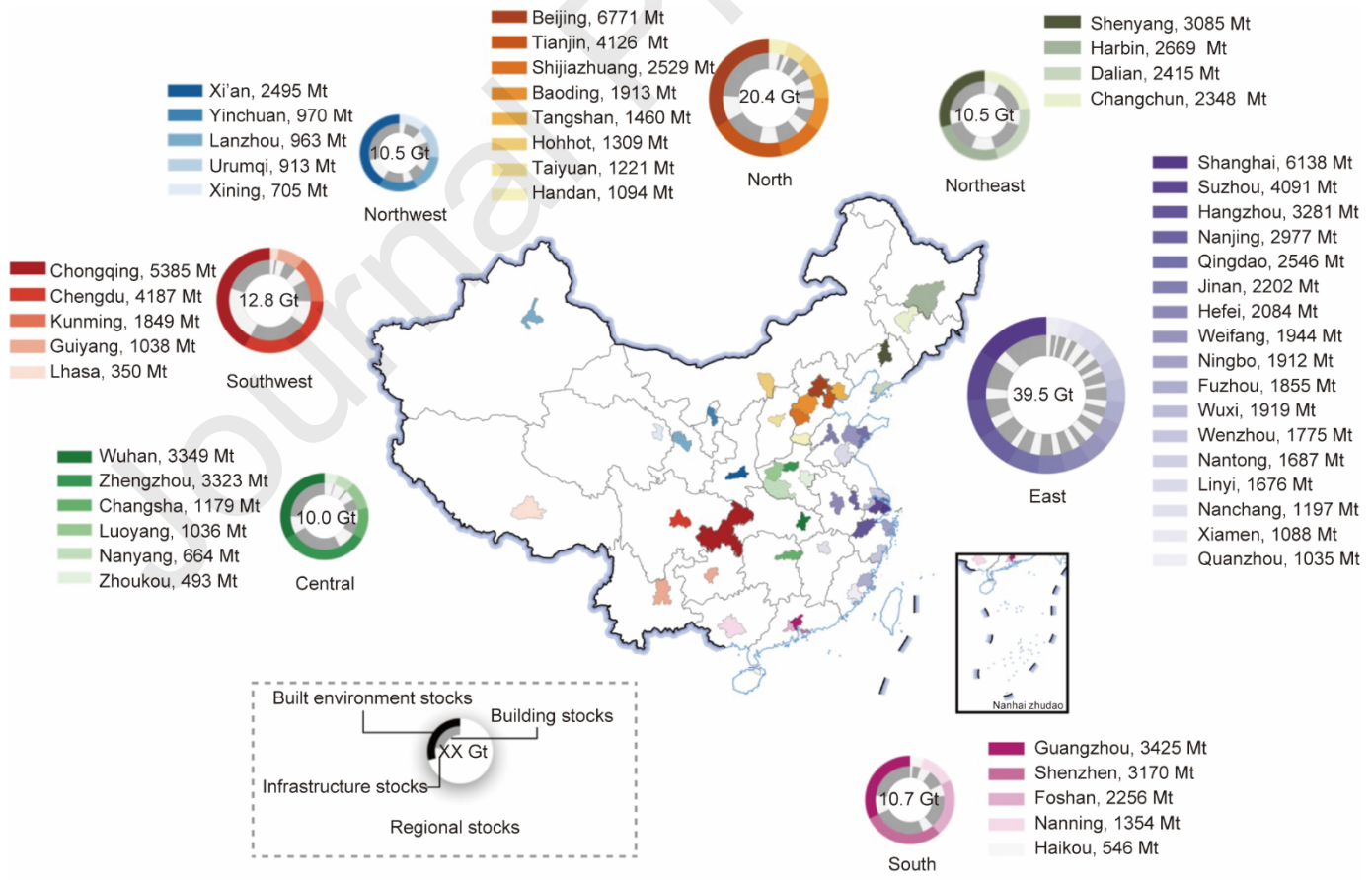

Fig. 2 Urban built environment stocks (total, buildings, and infrastructure) of the 50 selected cities in China. The seven colored wheels represent stocks aggregated by region (north, northeast, east, south, central, southwest, and northwest) accompanied by corresponding cities ranked by stock volume. The outer ring shows the total urban built environment stocks by city in this region, and the inner ring presents the ratio of building and infrastructure stocks in each city.

Statistically linear trends between the urban built environment stocks and socioeconomic factors confirm that cities with larg[illegible]aller and poorer cities (Figs. S12–14). This is also reflected by the fact that the urban built environment stocks tended to increase with an increasing tier rank and urbanization rate after categorizing the 50 cities into 6 tiers (first, new-first, second, third, fourth, and fifth) using an official classification system based on urban development factors including commercial vitality, transportation convenience, resident activity, lifestyle diversity, and future adaptability (Fig. S11). In this context, megacities with lower stocks per capita (such as 174 $t \cdot cap^{-1}$ in Chongqing), per square meters built-up area (such as 2.8 $t \cdot m^{-2}$ in Guangzhou), and per GDP (such as 1.3 $kg \cdot CNY^{-1}$ in Shenzhen) may have various sustainable paths of stock accumulation and socioeconomic growth that deserves more in-depth analysis to identify leapfrogging opportunities for other yet-to-be developed cities in China and beyond.

The urban form reflecting the physical layouts, structures, and functions of a city is an important driver of the varying levels of material stocks in the urban built environment [52]. Most construction materials were stocked in residential (43%) and industrial (22%) areas, followed by commercial (18%), public (14%) and infrastructure (4%) areas on average across the 50 cities (Fig. 2(a)). However, these proportions vary by city according to their socioeconomic characteristics. For example, Beijing is the capital of China and has the largest share (31%) of stock in public areas (such as education, culture, and healthcare). Meanwhile, Quanzhou and Foshan are two important manufacturing cities in south China that have the largest share of stocks in industrial areas at 52% and 47%, respectively. Furthermore, the variations between material stocks and land areas in different land-use categories clearly reveal the role of urban forms in determining built environment stocks. For example, an average commercial area (often dense and high-rise) accounts for only 3% of land use, but contributes 18% of the total stock, whereas public areas are often sparse and low, account for 49% of land use, but only contribute 14% of the total stock (Figs. 3(a) and (b)).

The building-to-road (BtR) stock ratio in China (5.47 on average for all 50 cities) is notably higher than that in European cities (3.45 in Salford Quays in Manchester [25], 3.13 in Odense city center [12], and 2.94 in Gothenburg [53]) and industrialized counties (1.65 in Japan [54], 1.12 in Germany [55], and 0.91 in Austria [56]). This result of lower road network densities is in line with earlier findings on the city [57] and national [58] levels in China and suggests that China's urban expansion tends to be more "vertical" than "horizontal." Further road and infrastructure development, particularly in residential and commercial areas, through better spatial planning or smart design and integration of buildings and roads has become an urgent need to optimize urban services and residents' well-being (Fig. 3)) [59]. Spatially, larger BtR ratio grids were mostly located in city centers, while lower value grids were found in city outskirts; the BtR ratio at the grid level was identified following a log-normal distribution across cities (Supplementary Fig. S21).

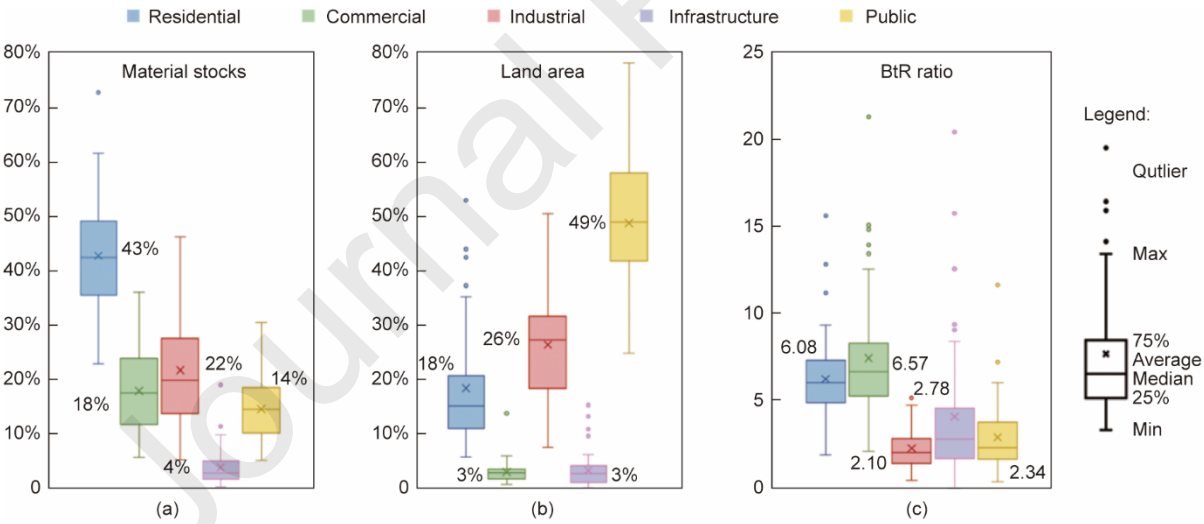

Fig. 3 Statistical distribution of built environment stock related values across cities by land use categories. (a) Shares of stocks, (b) shares of land areas, and (c) building to road (BtR) ratios. Stocks were calculated as an aggregation of stock values on the 500 m × 500 m grid level (Supplementary Material Section S3.6). The dominant type with the largest shared area is applied to the entire grid if a grid has several land use typologies (Section S1.5).

3.2 Patterns of spatially refined urban built environment stocks within cities

The gridded building material stocks were clustered in groups of patches using a density-based clustering algorithm when presented at a high spatial resolution on the 500 m × 500 m grid level [41] that detects categories based on the closeness of spatial distribution. In contrast, infrastructure material stocks generally follow the distribution of road lines and are spread throughout the city. Furthermore, the spatial patterns of building material stocks in Chinese cities suggest that there are three major phases of urban development: monocentric concentration, multicentric dispersion, and multicentric concentration.

Table 1 and Supplementary Table S23 present the spatial characteristics (number of clusters, dispersion index (DI) of clusters, and Gini index of building material stocks) of the three phases of building material stock growth as the average per capita GDP of cities increases from 70 649, 105 964, and 120 403 CNY, respectively. Fig. 4 shows such spatial patterns in

representative case cities (Nanyang, Chongqing, Zhengzhou, and Beijing).

• ities experiencing a monocentric concentration phase), and a limited number of top building stock grids are compactly distributed in this city with a relatively low dispersion index (DI = 9, Fig. 4(a))

• An increasing number of grids with large building stocks emerge on the outskirts of urban areas as cities continue to develop and accumulate materials in current grids (as new urban districts and satellite towns). Such multicentric-dispersion phases are featured by spreading clusters (increasing from 2 to 28) and growing dispersion index (increasing from 20 to 221) and can be observed in 22 cities (exemplified by Chongqing and Zhengzhou in Figs. 4(b) and (c), respectively).

• The growing urban built environment stocks gradually help ease communication and mobility in cities by upgrading transportation and telecommunications, attracting more population and businesses, and boosting the urban economy [60]. Accordingly, construction activities and building stock clusters emerge in subsidiary centers that link the central and outskirt clusters. Seventeen cities were identified in this multicentric concentration phase with a closer distance between building stock clusters (DI under 20), including Beijing (Fig. 4(d)).

Table 1
Spatial characteristics of building material stocks on 500 m fine-grained levels of the 50 Chinese cities.

Categories	Properties	Number of cities	Number of clusters	Dispersion index	Gini index	GDP per capita (CNY)
Monocentric-concentration	Cluster = 1 or Cluster ≥ 2 and DI < 20	11	1 (1–2)	9 (2–21)	0.58 (0.4–0.76)	70 609
Multicentric-dispersion	Cluster > 2 and DI ≥ 20	22	11 (2–28)	70 (20–221)	0.65 (0.45–0.79)	105 964
Multicentric-concentration	Cluster > 2 and DI < 20	17	9 (3–25)	13 (9–19)	0.58 (0.46–0.64)	120 403

The 11 cities at the monocentric-concentration phase are Guiyang, Haikou, Handan, Lanzhou, Lhasa, Linyi, Nanchang, Nanyang, Urumqi, Xining, and Zhoukou; the 22 cities at the multicentric-dispersion phase are Baoding, Changsha, Chongqing, Dalian, Foshan, Fuzhou, Harbin, Hangzhou, Luoyang, Nanning, Nantong, Ningbo, Qingdao, Quanzhou, Shijiazhuang, Suzhou, Tangshan, Weifang, Wenzhou, Wuxi, Yinchuan, and Zhengzhou; and the 17 cities at the multicentric-concentration phase are Beijing, Changchun, Chengdu, Guangzhou, Hefei, Hohhot, Jinan, Kunming, Nanjing, Shanghai, Shenyang, Shenzhen, Taiyuan, Tianjin, Wuhan, Xiamen, and Xi'an. The average values are shown for the number of clusters, dispersion index, and Gini index, with the ranges shown in parentheses.

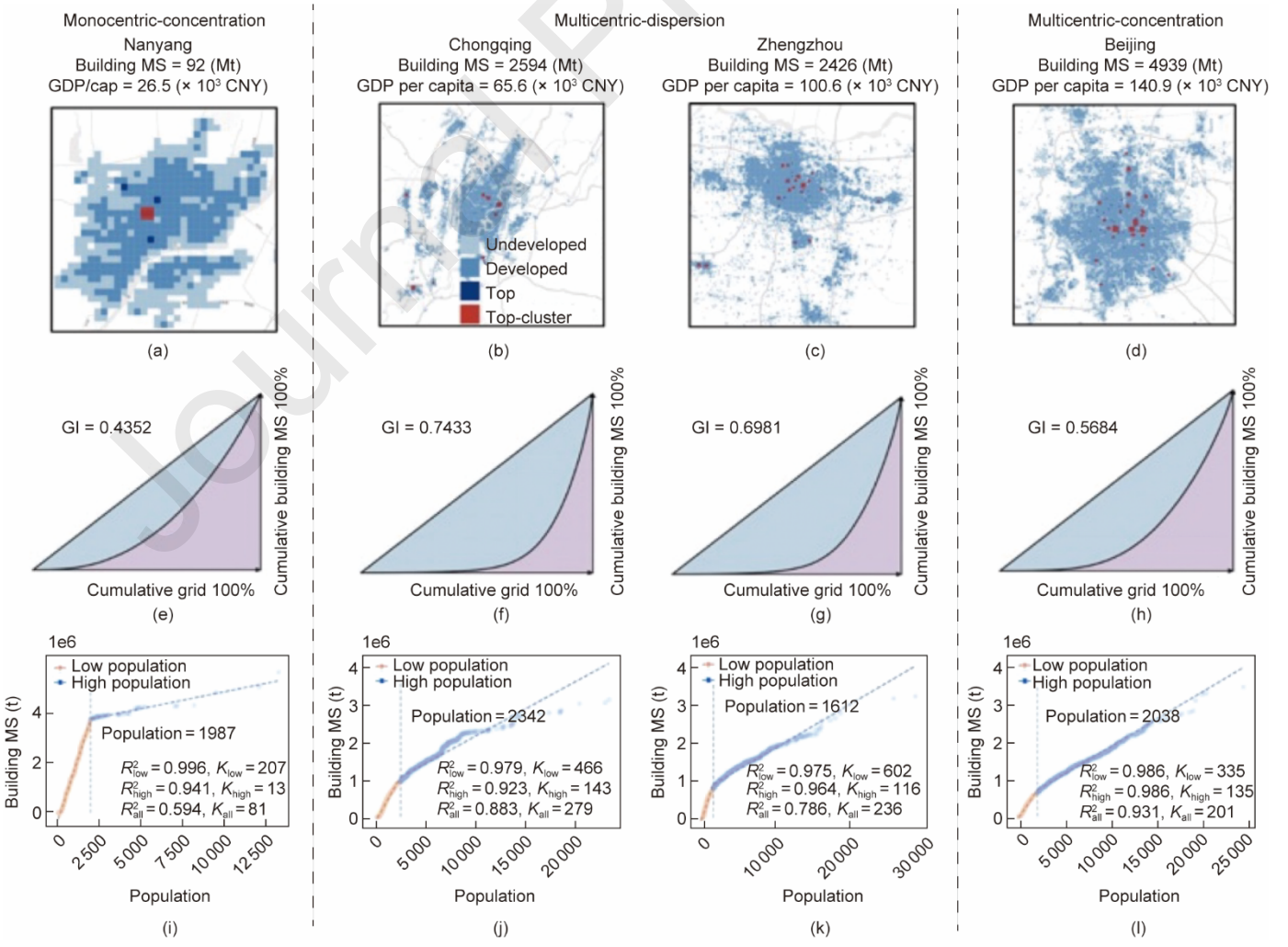

Fig. 4 Spatial patterns of building material stocks on 500 m fine-grained levels exemplified by Nanyang, Chongqing, Zhengzhou, and Beijing. (a–d) [redacted] stock grids), top (the top 1% of all urban stock grids), and top-cluster (the cluster of top grids) among building material stock grids, respectively (see Section S3.1 for details of grid classification). (e–h) The Gini index (GI) of building material stocks. (i–l) The two stages of linear correlations between building material stocks (with a break point) and population on the grid level ranked in ascending order. *K* represents the slope of different linear distributions.

Chinese cities demonstrate an "equilibrium–disequilibrium–equilibrium" pathway of building material stock development corresponding to the "concentration–dispersion–concentration" pattern observed above. This was initially shown in the changes in the Gini index values (average from 0.58, 0.65, and 0.58 for the three phases; Table 1 and Figs. 4(e)–(h)). Moreover, a two-parameter exponential distribution pattern was revealed for the building material stock growth of the 50 cities (exemplified by the probability density functions of Beijing, Suzhou, and Linyi in Fig. 5(a) and detailed for other cities in Supplementary Materials Section S3.4 and Appendix A.6).

The distribution of the 50 cities in the four quadrants defined by the location parameter (horizontally with an increasing proportion of low-stock grids) and the scale parameter (vertically with an increasing evenness of stock distribution) of their respective two-parameter exponential distributions are shown in Fig. 5(b). The cluster centers of cities in the monocentric-concentration phase (green star) and in the multicentric-concentration phase (orange star) appear in the second quadrant. This indicated a relatively uniform distribution of building material stocks. In contrast, the cluster center of cities in the multicentric-dispersion phase is located in the fourth quadrant. This represents a relatively uneven spatial distribution of building material stocks. The high number of cities with this disequilibrium status (22 out of 50) suggests an urgency for more optimized planning of urban built environment stocks and more coordinated development of urban and rural areas [61,62]. In this context, cities with higher, but more equalized built environment stocks (such as Changchun with eight clusters, 13 for DI, and 0.46 for GI) can shed light on stock accumulation pathways for other Chinese cities.

The spatially refined building material stocks and gridded population showed a linear correlation with a breakpoint for smaller population grids (R^2 = 0.98, on average) and larger ones (R^2 = 0.94, on average) in all 50 cities at 500 m resolution. These breakpoints are determined from the continuous piecewise linear function algorithm [63] and mostly vary between 1000 and 3000 for gridded populations—exemplified by Nanyang, Chongqing, Zhengzhou, and Beijing in Figs. 4(i)–(l) and detailed for other cities in Supplementary Material Section S3.5). That is, the stock growth rate in grids with a smaller population (K_{low} = 526) was significantly higher than that in grids with larger populations (K_{high} = 98). This implies that more materials were required in the initial stage of urbanization.

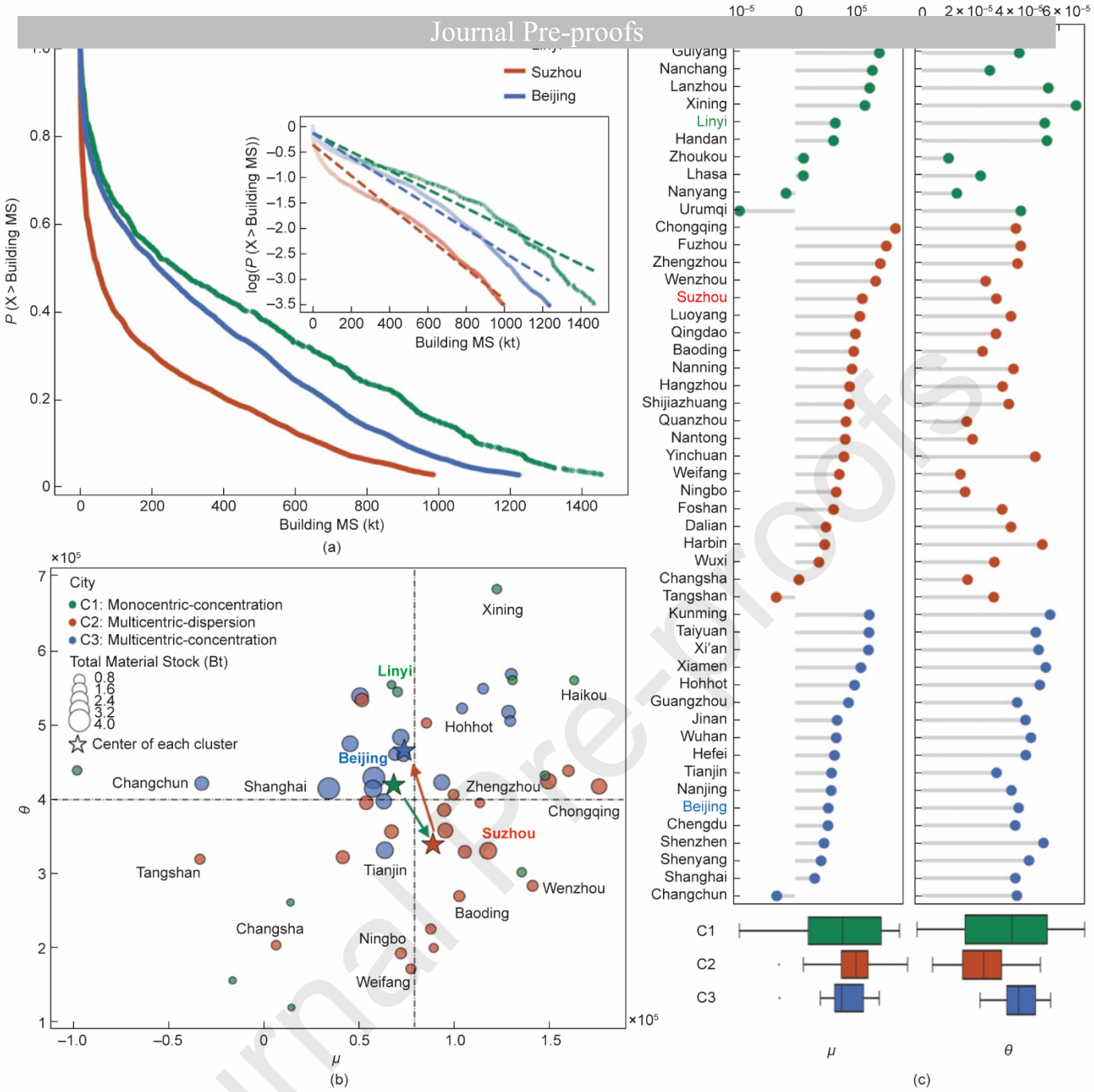

Fig. 5 Building material stock growth in Chinese cities following a two-parameter exponential distribution pattern. (a) The curves exemplified for Beijing, Suzhou, and Linyi; and (b–c) the location parameter μ that determines the transition along the horizontal axis and proportion of low stock grids and the scale parameter θ that refers to the slope chart level and evenness of stock distribution of the two-parameter exponential distribution curves across the 50 cities categorized by the three phases. The two dotted lines in (b) represent the mean values of μ and θ.

3.3 Discussion and implications

Our results reveal that the built environment stocks of many cities in China are close to or higher than those of mature cities in industrialized countries at the per capita level or per area level. This is in line with earlier findings on China's stock patterns of major construction materials such as cement [20,64] and aggregates [65] at the national level. Such patterns reflect the construction boom and real estate- and infrastructure-driven urbanization in the past decades in China. Many cities in China are building high-rise residential and non-residential buildings owing to their large population and increasingly limited land area, thus trading skylines for space. This suggests that understanding urban development from a physical stock perspective provides an important and complementary angle for characterizing and informing urbanization that is largely missing in the current literature on urbanization that focuses mostly on population growth [66] and land use change [67].

The spatially refined patterns of urban built environment stocks across and within cities clearly show the role of urban socioeconomic development, such as population and GDP, geomorphology, such as location and land area, and urban form, such as building-to-road ratio and land use structure, in determining the total volume and the sectoral and spatial distribution of stocks. Therefore, the pace of built environment construction, coordination of buildings and infrastructure development,

and tailored approaches for spatial planning and urban resource management should consider the varying stages of urban deve[illegible]n in western China and other cities in the world to bypass the disequilibrium stage and avoid spatial lock-ins, and provide the public, government, or industry stakeholders with insights into optimized urban spatial planning and urban system engineering towards smart resources, waste, and climate strategies and circular and low-carbon transitions of cities.

Such implications for urban system engineering primarily apply to resource and waste management perspectives. For example, high-resolution mapping of urban built environment stocks allows for an in-depth understanding of urban resource efficiency and forecasting of the quantity, composition, location, and value of future construction and demolition waste generation. Currently, construction and demolition waste in China is mostly dumped or landfilled with only 5% recycled [70]. This challenge will escalate considering the continued urbanization and construction boom in the foreseeable future in China. Understanding built environment stocks with a high spatiotemporal resolution provides a characterization of the urban resource cadaster [12] and enables the circular transition of cities [71]. This includes waste management and urban mining based on spatial and logistics optimization to minimize economic costs and maximize reuse and recycling.

Moreover, understanding the embodied climate impacts of urban built environment stocks facilitates discussions on accounting and mitigating GHG emission during the construction and operation of a city. The carbon replacement value (CRV) [72,73] concept was adopted to approximate the emissions of constructing a city that would be generated if the existing stock of a city was replaced using current technologies and materials. The overall CRV emissions of the 50 selected cities were estimated to be 32 Gt. This equals 60% of the global GHG emissions in 2019 [74] or 90% of the global CO_2 emissions in 2021 [75]. The CRV emissions in Beijing (2.29 Gt or 1.61 $t \cdot m^{-2}$), Shanghai (2.12 Gt or 2.12 $t \cdot m^{-2}$), Chengdu (1.33 Gt or 2.57 $t \cdot m^{-2}$), Suzhou (1.27 Gt or 2.75 $t \cdot m^{-2}$), and Tianjin (1.26 Gt or 1.25 $t \cdot m^{-2}$) are among the top five corresponding to the highest urban built environment stocks. This is much larger than those in European (such as 11 Mt in Odense [72]) and Australian (such as 24 Mt in Melbourne [76]) cities. Urban built environment stocks are essential to provide residents with basic services. The CRV emissions in these 50 cities can be used as a benchmark for the climate quota of the other 287 prefecture-level cities in China to reach the same level of services. Relatively low operational emissions and high CRV emissions were observed in two cities that dominate high technology and service-based economies: Shenzhen and Chengdu. In this context, cities with developed economies, upgraded industry structures, low operational emissions, low built environment stocks, and low CRV emissions (for example, Changsha, Quanzhou, Nantong, and Xiamen in the third quadrant of Supplementary Material Fig. S22) may be regarded as a model for the low-carbon transition of other small and medium-sized cities in China and beyond. At least 251 Gt of construction materials equaling 71 Gt of CRV emissions (or approximately seven times the current annual carbon emissions of China [77]) is needed for China's further urban expansion, assuming that the correlations between urban built environment stocks and socioeconomic parameters (Figs. S12–14) are applicable to the other 287 cities. Therefore, mitigation strategies ranging from technological innovations for emission-intensive construction materials (particularly steel [78] and cement [79]) to improving material efficiency [80], prolonging the building lifetime [30], and optimizing spatial planning [81] are urgently required to reduce the emissions of constructing a city. All these should be included in future model development and policy formulation from an urban system engineering perspective for the circular and low-carbon transition of cities.

3.4 Method validation and limitations

The proposed machine learning method offers a swift and effective approach for approximating urban material stocks when data incompleteness hinders traditional methods of building stock calculations. Four cross-validation approaches were designed to validate the proposed model and explore the consequent uncertainties (Supplementary Material Section S2.2). The prediction errors of the model were 0.23%, 3.79%, 0.119%, and 0.02% in the four different validation sets. This indicated that this grid-based method performs well in predicting building material stocks regardless of the city. The composition of building materials differs to some extent in northern and southern China owing to the different demands for winter heating. However, the large number of grid samples, together with our three sampling cities covering the north (Beijing) and south (Guangzhou and Shenzhen) allow the machine learning model to map building attributes to stock values in the sampling cities and make accurate predictions in other cities.

A comparison of our aggregated city-level building stock results for 2018 with a bottom-up accounting study [82] showed that the average differences were below 20% (2.59 Gt vs. 3.46 Gt for Chongqing, 4.19 Gt vs. 4.75 Gt for Shanghai, and 3.46 Gt versus 2.78 Gt for Tianjin). We believe that the building archetype classification and reference year may contribute to these differences. Furthermore, the building stock results in our study are significantly higher than those of two other studies in a few Chinese cities [27,37]. This gap is mainly related to the different years of estimation (2018 in this study vs. 2010 in previous literature) and the underestimation of nonresidential building stocks in these two studies (see Table S19). Overall, our study provides the first quantification of urban built environment stocks across and within cities on a large scale (50 cities).

The proposed machine learning method helped approximate urban material stocks across and within cities with overall good modelling performance. However, some limitations should be acknowledged. First, the absolute stock results bear unavoidable uncertainties and limitations owing to data gaps. Ideally, MCI data should be specific to each building or transportation infrastructure. We collected over 2000 building samples constructed from 1963–2020 and used the mean value to derive the MCIs for different building typologies. This per square meter indicator is very convenient to scale up, but does not linearly scale with the floor area. For example, a lower material intensity was identified in large-area buildings compared

with smaller buildings [83]. More material intensities are required to withstand wind and earthquake loads with increasing buil[illegible]data collection process may introduce errors since building coverage may be incomplete, and the vector maps of buildings and infrastructure may differ from reality, leading to uncertainties in the results. The performance of the machine learning model can be compromised when handling materials such as ceramics and glass that have a lower percentage composition. Nevertheless, their effects were relatively negligible owing to their insignificant contributions to the overall quantity. Finally, we used the process-based emission factors from Carbon Emission Accounts and Datasets (CEADs) and the Chinese Life Cycle Database (CLCD) for the CRV calculation using eBalance software. This does not cover the environmental impacts associated with supply chains. Therefore, our CRVs may be underestimated owing to truncation errors [85] in emission accounting. Overall, this study provides the first large-scale quantification of urban built environment stocks, although these limitations should be considered when interpreting the results.

4. Conclusions

Multi-source big geodata, machine learning, and bottom-up stock accounting were leveraged to characterize the built environment stocks of 50 selected cities in China at 500 m fine-grained levels. This large-scale empirical analysis helped to reveal considerable disparities in stocks across Chinese cities owing to their varying socioeconomic, geomorphological, and urban form characteristics. In particular, building material stock development in Chinese cities appeared to follow a two-parameter exponential distribution pattern and a concentration–dispersion–concentration pathway. Our results offer an important, yet hitherto largely missing stock perspective for characterizing and informing urbanization. This informs urban planners and policy makers on spatial planning, and facilitates urban system engineering towards the circular and low-carbon transition of cities. The modeling framework could be extended and validated using more cities to shed more light on future urbanization in China and in other countries.

Acknowledgments

This work is financially supported by the National Natural Science Foundation of China (71991484, 42271471, 72088101, and 41830645), Danish Agency for Higher Education and Science (International Network Project, 0192-00056B), and the Fundamental Research Funds for the Central Universities (Peking University). We acknowledge invaluable comments from Professor Michael F. Goodchild of University of California, Santa Barbara, on an earlier draft of this manuscript.

Author contributions

Zhou Huang and Gang Liu conceived the idea. Zhou Huang, Huadong Guo, and Gang Liu supervised the research. Yi Bao, Han Wang, Ganmin Yin, Lin Wan, Houji Qi, Qiaoxuan Li, and Hongzhao Tang contributed to geodata collection, analysis, and validation. Qiance Liu, Ruichang Mao, and Gang Liu compiled the building and infrastructure material composition data. Zhou Huang, Yi Bao, and Ruichang Mao run the simulation and drew the figures. Linna Li, Bailang Yu, Qinghua Guo, Yu Liu, and Huadong Guo contributed to discussion of results. Gang Liu, Ruichang Mao, Yi Bao, and Zhou Huang drafted the paper; and all authors analyzed the results and contributed to writing this paper.

Compliance with ethics guidelines

Zhou Huang, Yi Bao, Ruichang Mao, Han Wang, Ganmin Yin, Lin Wan, Houji Qi, Qiaoxuan Li, Hongzhao Tang, Qiance Liu, Linna Li, Bailang Yu, Qinghua Guo, Yu Liu, Huadong Guo, and Gang Liu declare that they have no conflict of interest or financial conflicts to disclose.

References

[1] Kalnay E, Cai M. Impact of urbanization and land-use change on climate. Nature 2003;423(6939):528–31.
[2] Montgomery MR. The urban transformation of the developing world. Science 2008;319(5864):761–4.
[3] United Nations Department of Economic and Social Affairs. 68% of the world population projected to live in urban areas by 2050, says UN [Internet]. New York City: United Nations Department of Economic and Social Affairs; 2018 May 16 [cited 2023 May 17]. Available from: https://www.un.org/development/desa/en/news/population/2018-revision-of-world-urbanization-prospects.html.
[4] Liu T, Qi Y, Cao G, Liu H. Spatial patterns, driving forces, and urbanization effects of China's internal migration: county-level analysis based on the 2000 and 2010 censuses. J Geogr Sci 2015;25(2):236–56.
[5] Liu T, Liu H, Qi Y. Construction land expansion and cultivated land protection in urbanizing China: insights from national land surveys, 1996–2006. Habitat Int 2015;46:13–22.
[6] Zhong X, Hu M, Deetman S, Steubing B, Lin HX, Hernandez GA, et al. Global greenhouse gas emissions from residential and commercial building materials and mitigation strategies to 2060. Nat Commun 2021;12(1):6126.
[7] Jiang M, Behrens P, Wang T, Tang Z, Yu Y, Chen D, et al. Provincial and sector-level material footprints in China. Proc Natl Acad Sci USA 2019;116(52):26484–90.
[8] Creutzig F, Niamir L, Bai X, Callaghan M, Cullen J, Díaz-José J, et al. Demand-side solutions to climate change mitigation consistent with high levels of well-being. Nat Clim Chang 2022;12(1):36–46.
[9] Chen S, Chen B, Feng K, Liu Z, Fromer N, Tan X, et al. Physical and virtual carbon metabolism of global cities. Nat Commun 2020;11(1):182.
[10] Zhong X, Deetman S, Tukker A, Behrens P. Increasing material efficiencies of buildings to address the global sand crisis. Nat Sustain 2022;5(5):389–

92.
[11] ... fifth assessment report of the Intergovernmental Panel on Climate Change. New York City: Cambridge University Press; 2014.
[12] Lanau M, Liu G. Developing an urban resource cadaster for circular economy: a case of Odense, Denmark. Environ Sci Technol 2020;54(7):4675–85.
[13] Kennedy CA, Stewart I, Facchini A, Cersosimo I, Mele R, Chen B, et al. Energy and material flows of megacities. Proc Natl Acad Sci USA 2015;112(19):5985–90.
[14] World Green Building Council. New report: the building and construction sector can reach net zero carbon emissions by 2050. Report. London: World Green Building Council; 2019 Sep 23.
[15] Watts M. Cities spearhead climate action. Nat Clim Chang 2017;7(8):537–8.
[16] Duan H, Li J, Liu G. Growing threat of urban waste dumps. Nature 2017;546:599.
[17] Nagendra H, Bai X, Brondizio ES, Lwasa S. The urban south and the predicament of global sustainability. Nat Sustain 2018;1(7):341–9.
[18] Wang T, Müller DB, Graedel TE. Forging the anthropogenic iron cycle. Environ Sci Technol 2007;41(14):5120–9.
[19] Müller DB, Wang T, Duval B, Graedel TE. Exploring the engine of anthropogenic iron cycles. Proc Natl Acad Sci USA 2006;103(44):16111–6.
[20] Cao Z, Shen L, Løvik AN, Müller DB, Liu G. Elaborating the history of our cementing societies: an in-use stock perspective. Environ Sci Technol 2017;51(19):11468–75.
[21] Heeren N, Hellweg S. Tracking construction material over space and time: prospective and geo-referenced modeling of building stocks and construction material flows. J Ind Ecol 2019;23(1):253–67.
[22] Mao R, Bao Y, Duan H, Liu G. Global urban subway development, construction material stocks, and embodied carbon emissions. Humanit Soc Sci Commun 2021;8(1):83.
[23] Liu Q, Cao Z, Liu X, Liu L, Dai T, Han J, et al. Product and metal stocks accumulation of China's megacities: patterns, drivers, and implications. Environ Sci Technol 2019;53(8):4128–39.
[24] Huang C, Han J, Chen WQ. Changing patterns and determinants of infrastructures' material stocks in Chinese cities. Resour Conserv Recycling 2017;123:47–53.
[25] Tanikawa H, Hashimoto S. Urban stock over time: spatial material stock analysis using 4D-GIS. Build Res Inform 2009;37(5-6):483–502.
[26] Lanau M, Liu G, Kral U, Wiedenhofer D, Keijzer E, Yu C, et al. Taking stock of built environment stock studies: progress and prospects. Environ Sci Technol 2019;53(15):8499–515.
[27] Guo J, Miatto A, Shi F, Tanikawa H. Spatially explicit material stock analysis of buildings in Eastern China metropoles. Resour Conserv Recycling 2019;146:45–54.
[28] Takahashi KI, Terakado R, Nakamura J, Adachi Y, Elvidge CD, Matsuno Y. In-use stock analysis using satellite nighttime light observation data. Resour Conserv Recycling 2010;55(2):196–200.
[29] Bai X, Shi P, Liu Y. Society: realizing China's urban dream. Nature 2014;509(7499):158–60.
[30] Cao Z, Liu G, Duan H, Xi F, Liu G, Yang W. Unravelling the mystery of Chinese building lifetime: a calibration and verification based on dynamic material flow analysis. Appl Energy 2019;238:442–52.
[31] Hong L, Zhou N, Feng W, Khanna N, Fridley D, Zhao Y, et al. Building stock dynamics and its impacts on materials and energy demand in China. Energy Policy 2016;94:47–55.
[32] Wang H, Lu X, Deng Y, Sun Y, Nielsen CP, Liu Y, et al. China's CO2 peak before 2030 implied from characteristics and growth of cities. Nat Sustain 2019;2(8):748–54.
[33] Mao R, Duan H, Dong D, Zuo J, Song Q, Liu G, et al. Quantification of carbon footprint of urban roads via life cycle assessment: case study of a megacity-Shenzhen, China. J Clean Prod 2017;166:40–8.
[34] Wang T, Zhou J, Yue Y, Yang J, Hashimoto S. Weight under steel wheels: material stock and flow analysis of high-speed rail in China. J Ind Ecol 2016;20(6):1349–59.
[35] Guo Z, Hu D, Zhang F, Huang G, Xiao Q. An integrated material metabolism model for stocks of urban road system in Beijing, China. Sci Total Environ 2014;470–471:883–94.
[36] Mao R, Bao Y, Huang Z, Liu Q, Liu G. High-resolution mapping of the urban built environment stocks in Beijing. Environ Sci Technol 2020;54(9):5345–55.
[37] Han J, Chen WQ, Zhang L, Liu G. Uncovering the spatiotemporal dynamics of urban infrastructure development: a high spatial resolution material stock and flow analysis. Environ Sci Technol 2018;52(21):12122–32.
[38] Guo J, Fishman T, Wang Y, Miatto A, Wuyts W, Zheng L, et al. Urban development and sustainability challenges chronicled by a century of construction material flows and stocks in Tiexi, China. J Ind Ecol 2021;25(1):162–75.
[39] Gong P, Chen B, Li X, Liu H, Wang J, Bai Y, et al. Mapping essential urban land use categories in China (EULUC-China): preliminary results for 2018. Sci Bull (Beijing) 2020;65(3):182–7.
[40] WorldPop. Global high resolution population denominators project - funded by the bill and melinda gates foundation [Internet]. Otara: WorldPop; 2020 Feb 01 [cited 2023 May 17]. Available from: https://www.worldpop.org/geodata/summary?id=24924.
[41] Ester M, Kriegel HP, Sander J, Xu X. A density-based algorithm for discovering clusters in large spatial databases with noise. In: Proceedings of the 2nd International Conference on Knowledge Discovery and Data Mining; 1996 Aug 2–4; Oregon, Portland. Cambridge: AAAI Press; 1996.
[42] United Nations Environment Programme (UNEP). Global resources outlook 2019: natural resources for the future we want. Report. Paris: International Resource Panel (IRP); 2019. Available from: https://www.resourcepanel.org/reports/global-resources-outlook.
[43] Kleemann F, Lederer J, Rechberger H, Fellner J. GIS-based analysis of Vienna's material stock in buildings. J Ind Ecol 2017;21(2):368–80.
[44] Miatto A, Schandl H, Forlin L, Ronzani F, Borin P, Giordano A, et al. A spatial analysis of material stock accumulation and demolition waste potential of buildings: a case study of Padua. Resour Conserv Recycling 2019;142:245–56.
[45] Streeck J, Wiedenhofer D, Krausmann F, Haberl H. Stock-flow relations in the socio-economic metabolism of the United Kingdom 1800–2017. Resour Conserv Recycling 2020;161:104960.
[46] Bai X, Chen J, Shi P. Landscape urbanization and economic growth in China: positive feedbacks and sustainability dilemmas. Environ Sci Technol 2012;46(1):132–9.
[47] Liu Z, Deng Z, He G, Wang H, Zhang X, Lin J, et al. Challenges and opportunities for carbon neutrality in China. Nat Rev Earth Environ 2021;3(2):141–55.
[48] Meng X, Long Y. Shrinking cities in China: evidence from the latest two population censuses 2010–2020. Environ Plann A 2022;54(3):449–53.
[49] Qi W, Liu S, Zhao M, Liu Z. China's different spatial patterns of population growth based on the "Hu Line". J Geogr Sci 2016;26(11):1611–25.
[50] Tan J, Lo K, Qiu F, Liu W, Li J, Zhang P. Regional economic resilience: resistance and recoverability of resource-based cities during economic crises in northeast China. Sustainability 2017;9(12):2136.
[51] Gao B, Huang Q, He C, Sun Z, Zhang D. How does sprawl differ across cities in China? A multi-scale investigation using nighttime light and census data. Landsc Urban Plan 2016;148:89–98.
[52] VandeWeghe JR, Kennedy C. A spatial analysis of residential greenhouse gas emissions in the Toronto Census Metropolitan Area. J Ind Ecol 2007;11(2):133–44.
[53] Gontia P, Thuvander L, Ebrahimi B, Vinas V, Rosado L, Wallbaum H. Spatial analysis of urban material stock with clustering algorithms: a Northern European case study. J Ind Ecol 2019;23(6):1328–43.
[54] Tanikawa H, Fishman T, Okuoka K, Sugimoto K. The weight of society over time and space: a comprehensive account of the construction material

stock of Japan, 1945–2010. J Ind Ecol 2015;19(5):778–791.
[55] S cling 2017;123:93–107.
[56] Daxbeck H, Buschmann H, Neumayer S, Brandt B. Methodology for mapping of physical stocks. Sixth framework programme priority. Austria: Resource Management Agency (RMA); 2009 Oct 6. Contract No.: 044409.
[57] Zhao G, Zheng X, Yuan Z, Zhang L. Spatial and temporal characteristics of road networks and urban expansion. Land (Basel) 2017;6(2):30.
[58] Hong J, Chu Z, Wang Q. Transport infrastructure and regional economic growth: evidence from China. Transportation 2011;38(5):737–52.
[59] Ameen RFM, Mourshed M, Li H. A critical review of environmental assessment tools for sustainable urban design. Environ Impact Assess Rev 2015;55:110–25.
[60] Thacker S, Adshead D, Fay M, Hallegatte S, Harvey M, Meller H, et al. Infrastructure for sustainable development. Nat Sustain 2019;2(4):324–31.
[61] Song Y. Rising Chinese regional income inequality: the role of fiscal decentralization. China Econ Rev 2013;27:294–309.
[62] Li KQ. Report on the work of the government [Internet]. Beiing: State Council of the People's Republic of China; 2019 May 16 [cited 2023 May 17]. Available from: https://english.www.gov.cn/premier/speeches/2019/03/16/content_281476565265580.htm.
[63] Jekel CF, Venter G. pwlf: a Python library for fitting 1D continuous piecewise linear functions [Internet]. Online: GetHub, Inc.; 2019 Feb 6 [cited 2023 May 17]. Available from: https://github.com/cjekel/piecewise_linear_fit_py.
[64] Cao Z, Myers RJ, Lupton RC, Duan H, Sacchi R, Zhou N, et al. The sponge effect and carbon emission mitigation potentials of the global cement cycle. Nat Commun 2020;11(1):3777.
[65] Ren Z, Jiang M, Chen D, Yu Y, Li F, Xu M, et al. Stocks and flows of sand, gravel, and crushed stone in China (1978–2018): evidence of the peaking and structural transformation of supply and demand. Resour Conserv Recycling 2022;180:106173.
[66] Buhaug H, Urdal H. An urbanization bomb? Population growth and social disorder in cities. Glob Environ Change 2013;23(1):1–10.
[67] Lai L, Huang X, Yang H, Chuai X, Zhang M, Zhong T, et al. Carbon emissions from land-use change and management in China between 1990 and 2010. Sci Adv 2016;2(11):e1601063.
[68] Elmqvist T, Andersson E, Frantzeskaki N, McPhearson T, Olsson P, Gaffney O, et al. Sustainability and resilience for transformation in the urban century. Nat Sustain 2019;2(4):267–73.
[69] York R, Rosa EA, Dietz T. STIRPAT, IPAT and ImPACT: analytic tools for unpacking the driving forces of environmental impacts. Ecol Econ 2003;46(3):351–65.
[70] Huang B, Wang X, Kua H, Geng Y, Bleischwitz R, Ren J. Construction and demolition waste management in China through the 3R principle. Resour Conserv Recycling 2018;129:36–44.
[71] Ajayebi A, Hopkinson P, Zhou K, Lam D, Chen HM, Wang Y. Spatiotemporal model to quantify stocks of building structural products for a prospective circular economy. Resour Conserv Recycling 2020;162:105026.
[72] Lanau M, Herbert L, Liu G. Extending urban stocks and flows analysis to urban greenhouse gas emission accounting: a case of Odense, Denmark. J Ind Ecol 2021;25(4):961–78.
[73] Müller DB, Liu G, Løvik AN, Modaresi R, Pauliuk S, Steinhoff FS, et al. Carbon emissions of infrastructure development. Environ Sci Technol 2013;47(20):11739–46.
[74] UNEP Copenhagen Climate Centre (UNEP-CCC). Emissions gap report 2020. Report. Copenhagen: UNEP Copenhagen Climate Centre; 2020 Dec 09.
[75] Liu Z, Deng Z, Davis SJ, Giron C, Ciais P. Monitoring global carbon emissions in 2021. Nat Rev Earth Environ 2022;3(4):217–9.
[76] Stephan A, Athanassiadis A. Quantifying and mapping embodied environmental requirements of urban building stocks. Build Environ 2017;114:187–202.
[77] Mi Z, Wei YM, Wang B, Meng J, Liu Z, Shan Y, et al. Socioeconomic impact assessment of China's CO2 emissions peak prior to 2030. J Clean Prod 2017;142:2227–36.
[78] Yu B, Li X, Qiao Y, Shi L. Low-carbon transition of iron and steel industry in China: carbon intensity, economic growth and policy intervention. J Environ Sci (China) 2015;28:137–47.
[79] Gao T, Shen L, Shen M, Liu L, Chen F, Gao L. Evolution and projection of CO2 emissions for China's cement industry from 1980 to 2020. Renew Sustain Energy Rev 2017;74:522–37.
[80] Dunant CF, Drewniok MP, Sansom M, Corbey S, Cullen JM, Allwood JM. Options to make steel reuse profitable: an analysis of cost and risk distribution across the UK construction value chain. J Clean Prod 2018;183:102–11.
[81] Wang SH, Huang SL, Huang PJ. Can spatial planning really mitigate carbon dioxide emissions in urban areas? A case study in Taipei, Taiwan. Landsc Urban Plan 2018;169:22–36.
[82] Song L, Han J, Li N, Huang Y, Hao M, Dai M, et al. China material stocks and flows account for 1978–2018. Sci Data 2021;8(1):303.
[83] Stephan A, Crawford RH. The relationship between house size and life cycle energy demand: implications for energy efficiency regulations for buildings. Energy 2016;116:1158–71.
[84] Helal J, Stephan A, Crawford RH. The influence of structural design methods on the embodied greenhouse gas emissions of structural systems for tall buildings. Structures 2020;24:650–65.
[85] Crawford RH, Stephan A, Prideaux F. The EPiC database: hybrid embodied environmental flow coefficients for construction materials. Resour Conserv Recycling 2022;180:106058.

Declaration of interests

☒ The authors declare that they have no known competing financial interests or personal relationships that could have appeared to influence the work reported in this paper.

☐The authors declare the following financial interests/personal relationships which may be considered as potential competing interests: